Electronic Supplementary Material (ESI) for Inorganic Chemistry Frontiers.

Supporting Information

Fabrication of 3D Heteroatom-Doped Porous Carbon Derived from Assembly of Chelate Foams via a Solid State Method

Yu Wang, Ying Pan, Liangkui Zhu, Ningning Guo, Runwei Wang*, Zongtao Zhang and Shilun Qiu

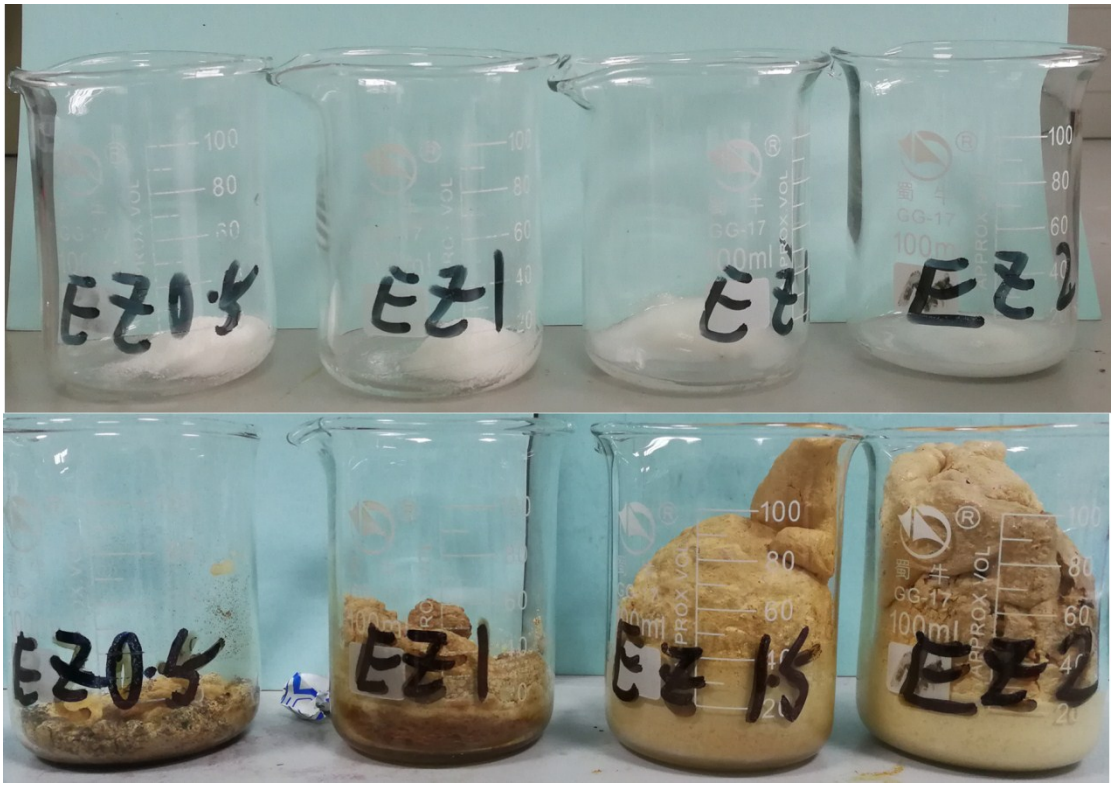

Fig. S1. Photographs of precursors (up) and 3D Chelates Foams(down) for EZ_x in 100mL glass beaker.

Fig. S2. Photographs of precursors (up) and 3D Chelates Foams(down) for DZ_x., $DZ_{0.5}$, DZ_1, $DZ_{1.5}$ are in 100mL glass beakers. DZ_2 in 100mL glass beaker. $DZ_{2.5}$ in 200mL glass beaker.

Fig. S3. Photographs of precursors (up) and 3D Chelates Foams (down) for NZ_x in 25 mL glass beakers.

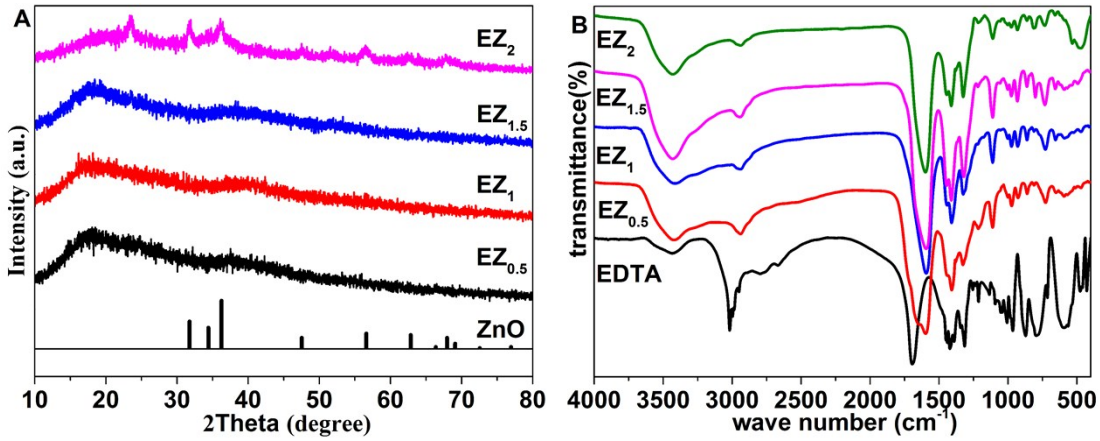

Figure S4. XRD (A) and IR (B) curves of EZ_X

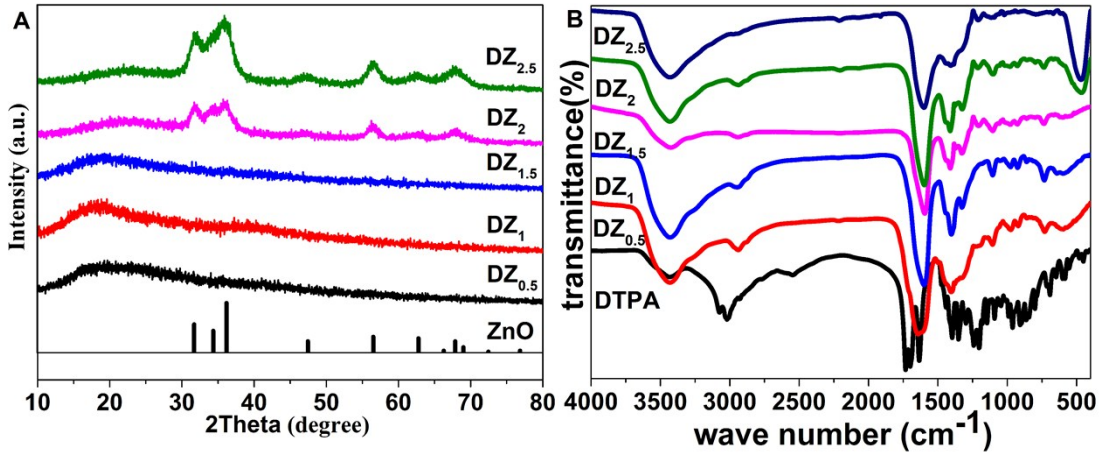

Figure S5. XRD (A) and IR (B) curves of DZ_X

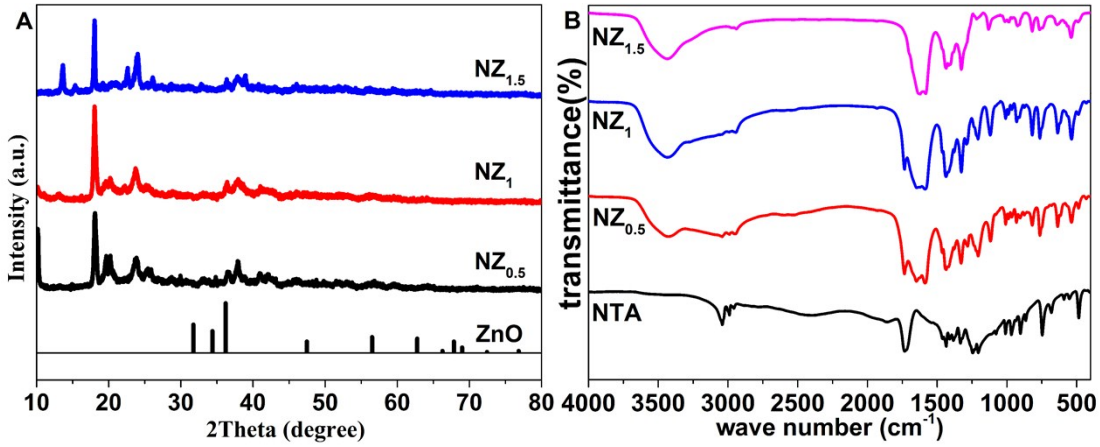

Figure S6. XRD (A) and IR (B) curves of NZ_X

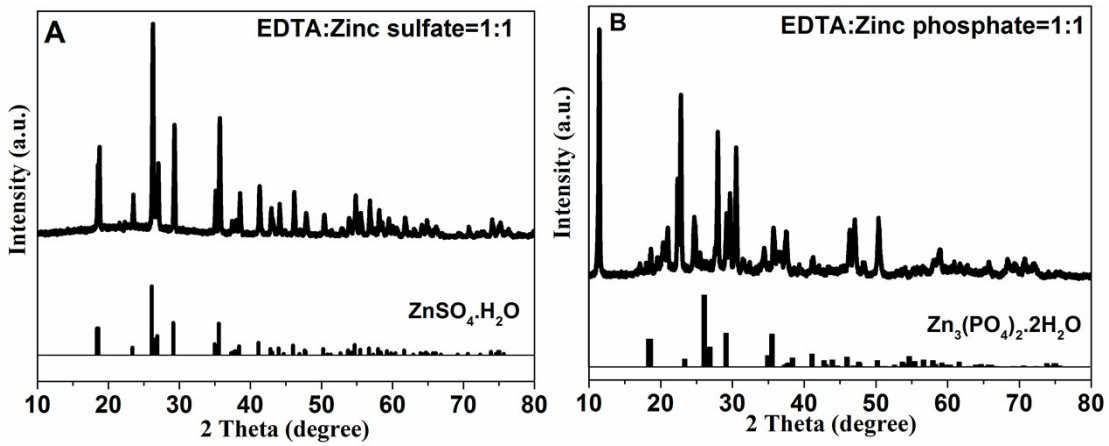

Figure S7. XRD results, (A) EDTA heated with Zinc sulfate. (B) EDTA heated with Zinc phosphate.

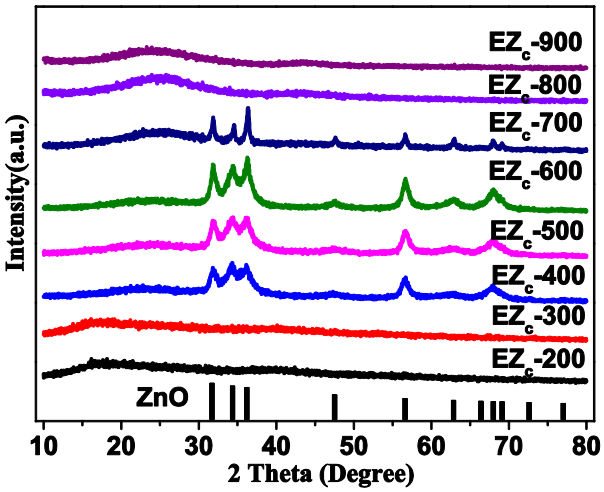

Figure S8. XRD result of EZ1 carbonized at different temperature.

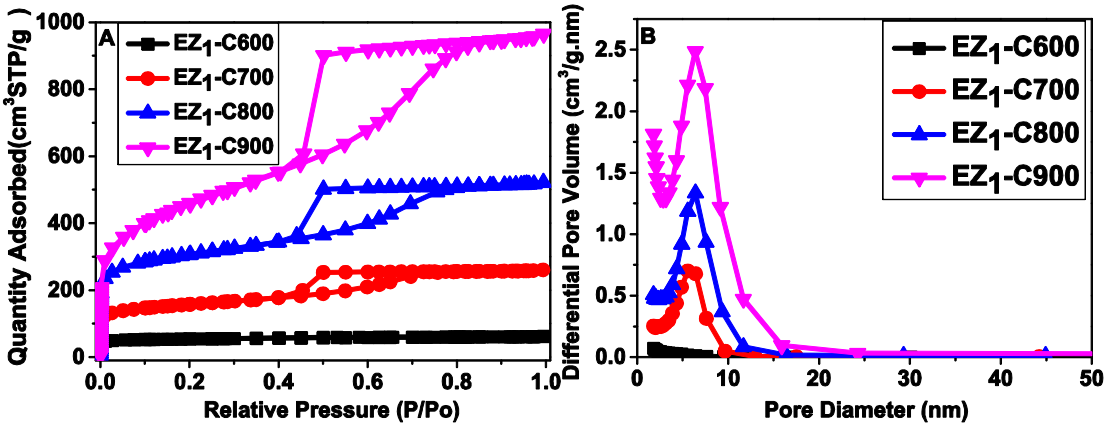

Figure S9. (A) N_2 adsorption isotherms of EZ_1 carbonized at different temperature and (B) corresponding pore size distribution.

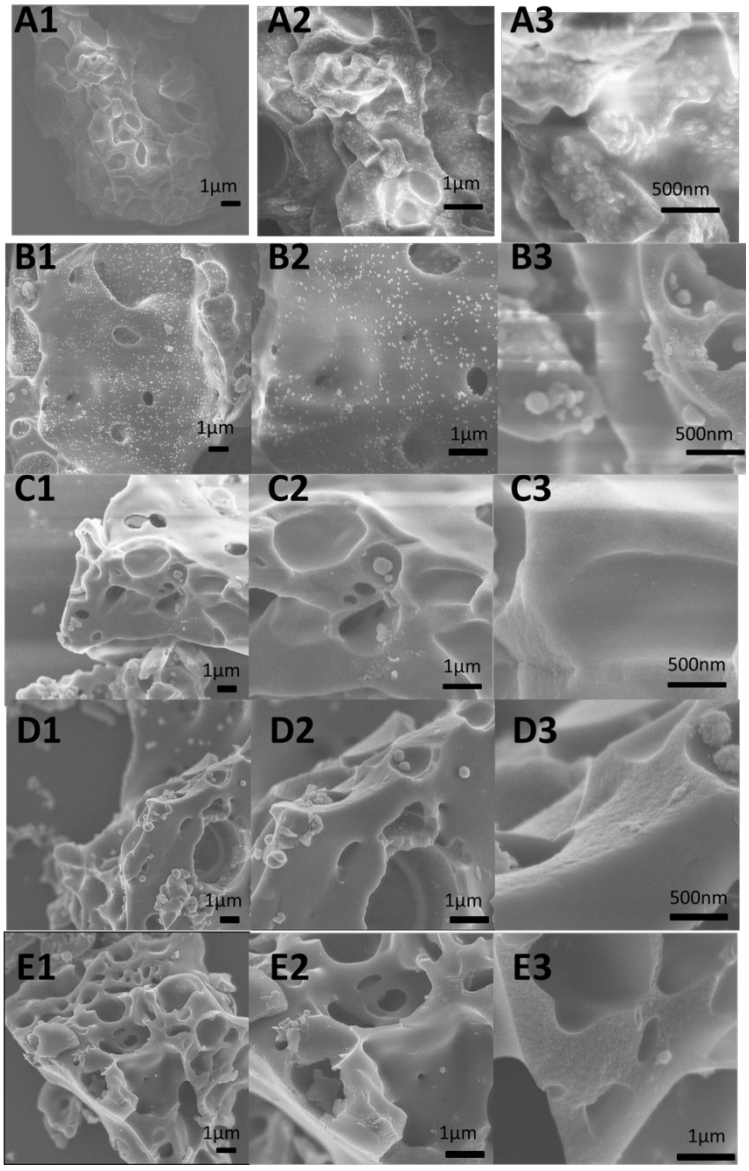

Figure S10. SEM images of (A1 - A3) EZ_1-C300, (B1 - B3) EZ_1-C400, (C1 - C3) EZ_1-C500, (D1- D3) EZ_1-C600, (E1 - E3) EZ_1-C700.

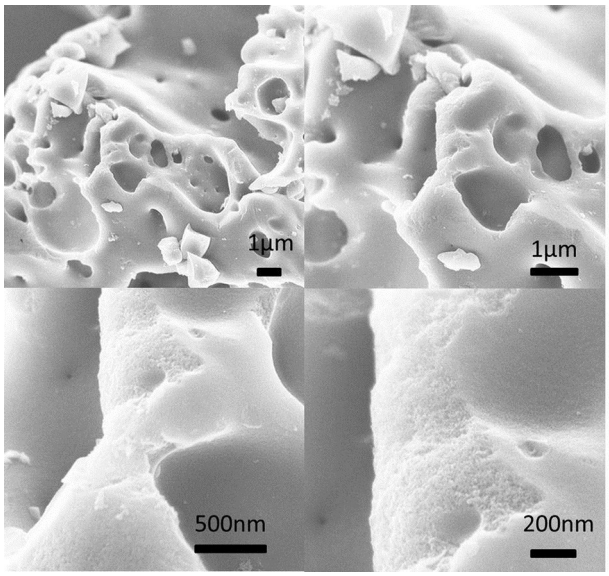

Figure S11. SEM images of EZ_1-C800

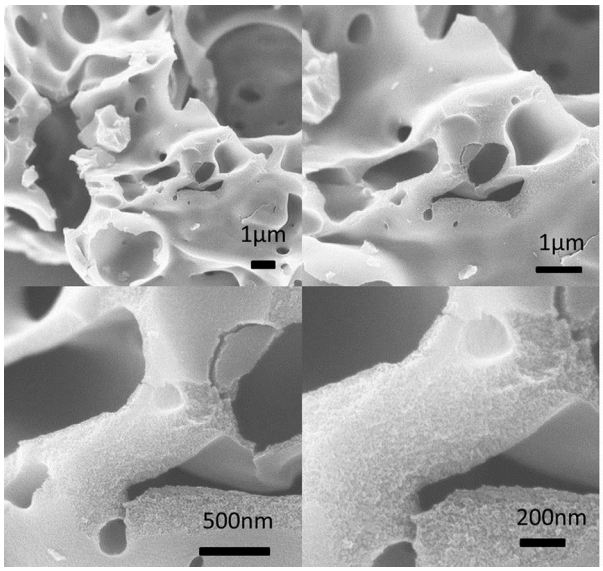

Figure S12. SEM images of EZ_1-C900

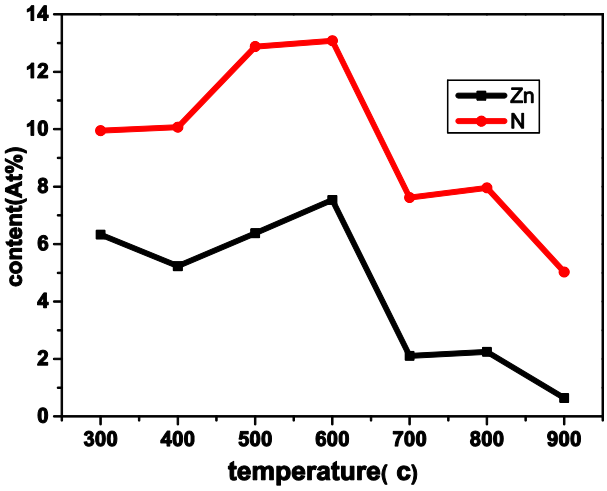

Figure S13. Nitrogen and Zn content for EZ_1-C from XPS result.

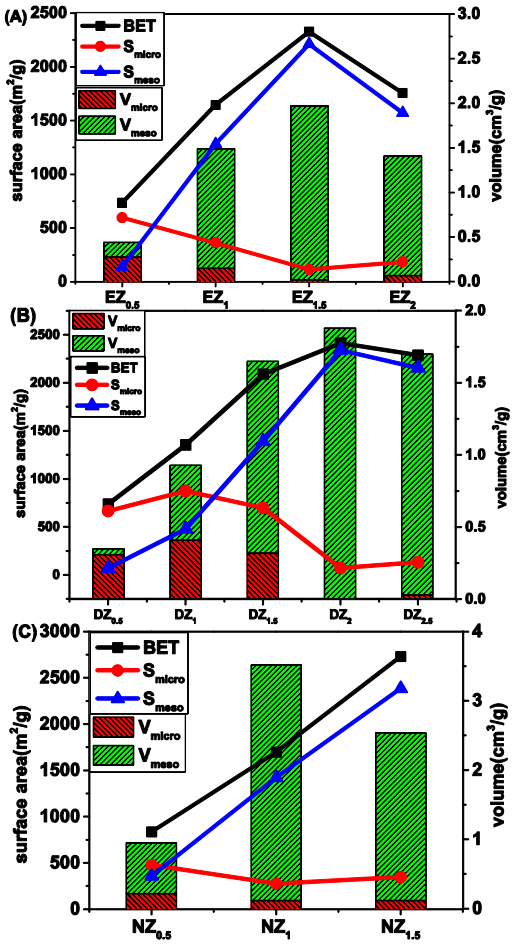

Figure S14. Porous structure parameters of NCFs. EZ_x-C (A1, A2), DZ_x-C (B1, B2) and NZ_x-C (C1, C2).

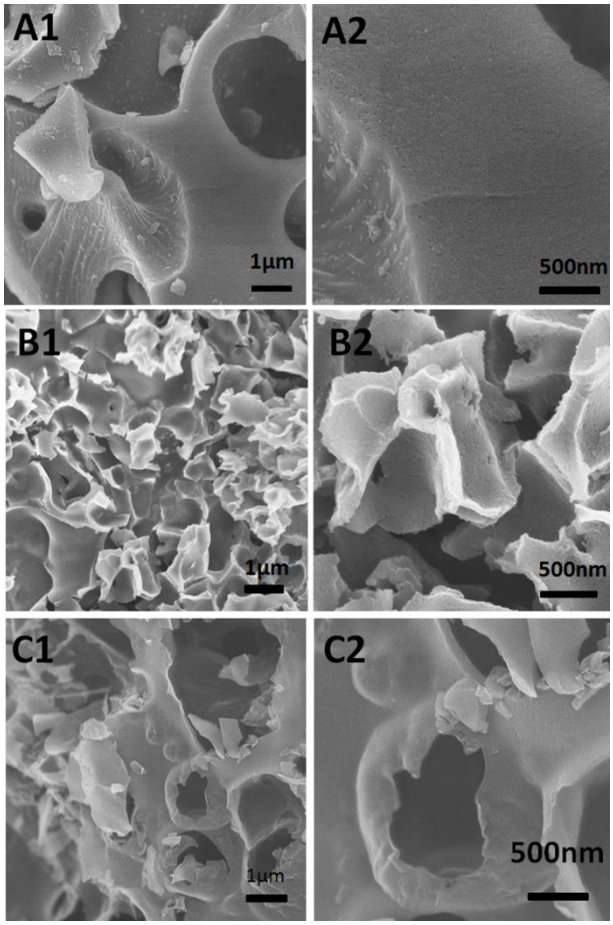

Figure S15. SEM images of $EZ_{0.5}$-C (A1, A2), $EZ_{1.5}$-C (B1, B2) and EZ_2-C (C1, C2).

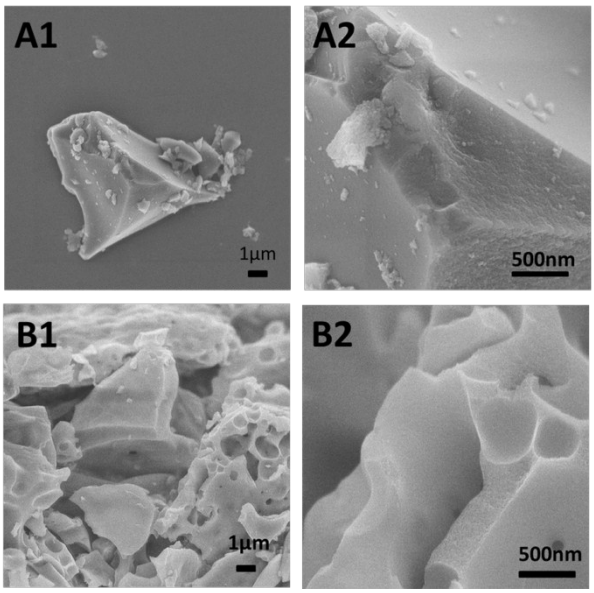

Figure S16. SEM images of $DZ_{0.5}$-C (A1, A2) and DZ_1-C (B1, B2).

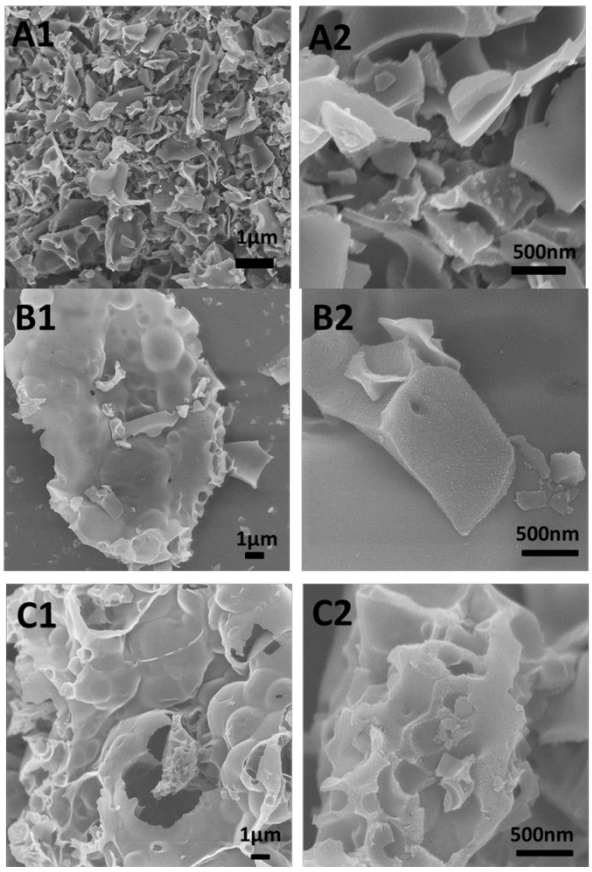

Figure S17. SEM images of $DZ_{1.5}$-C (A1, A2), DZ_2-C (B1, B2) and $DZ_{2.5}$-C (C1, C2).

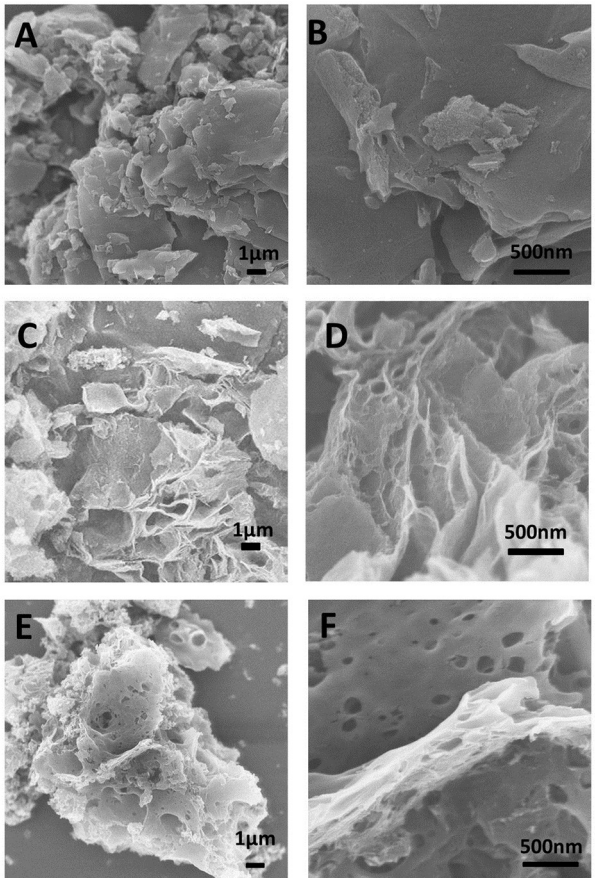

Figure S18. SEM images of $NZ_{0.5}$-C (A1, A2), NZ_1-C (B1, B2) and $NZ_{1.5}$-C (C1, C2).

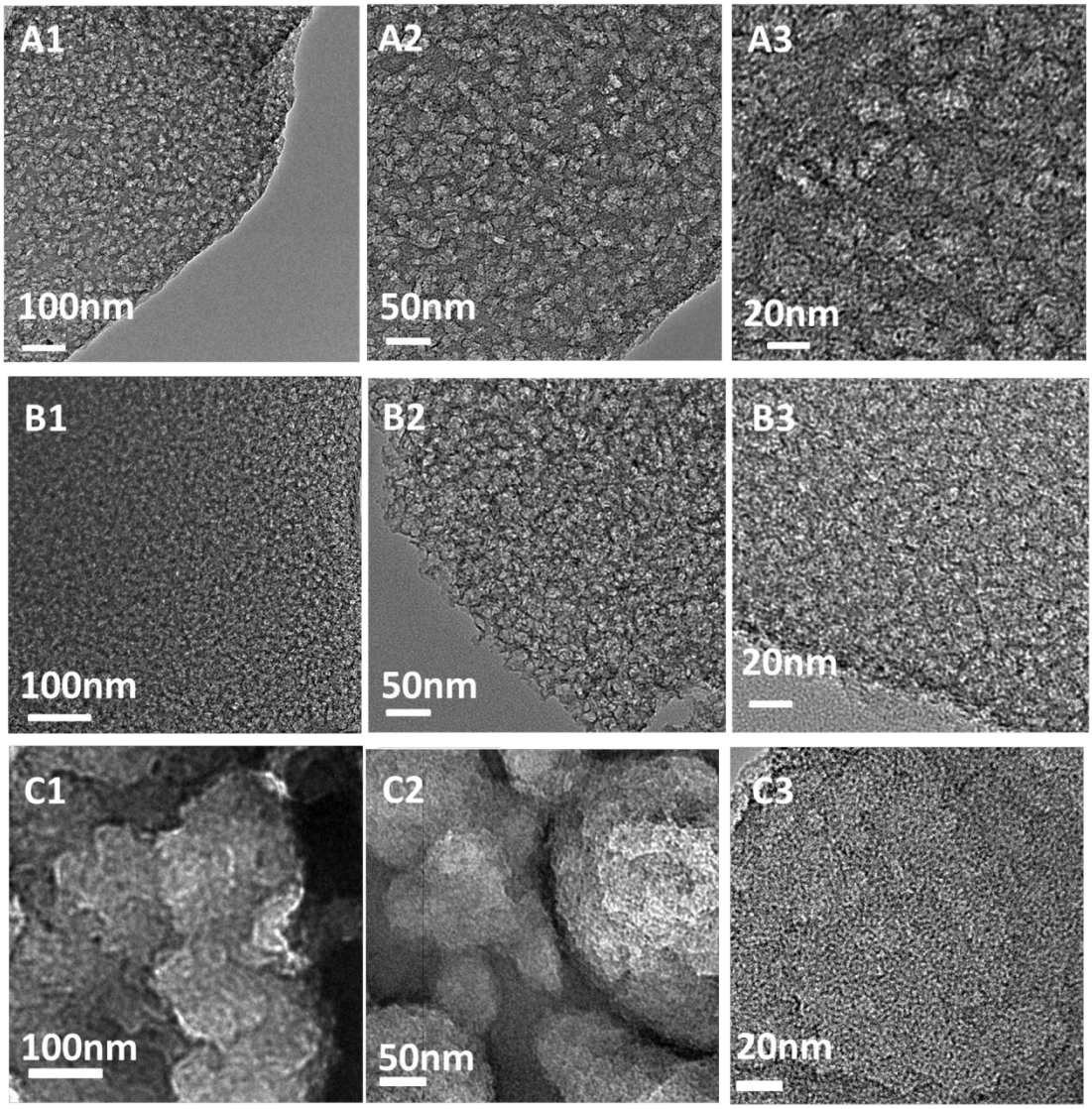

Figure S19. TEM images of $EZ_{0.5}$-C (A1, A2, A3), EZ_1-C (B1, B2, B3) and $EZ_{1.5}$-C (C1, C2, C3).

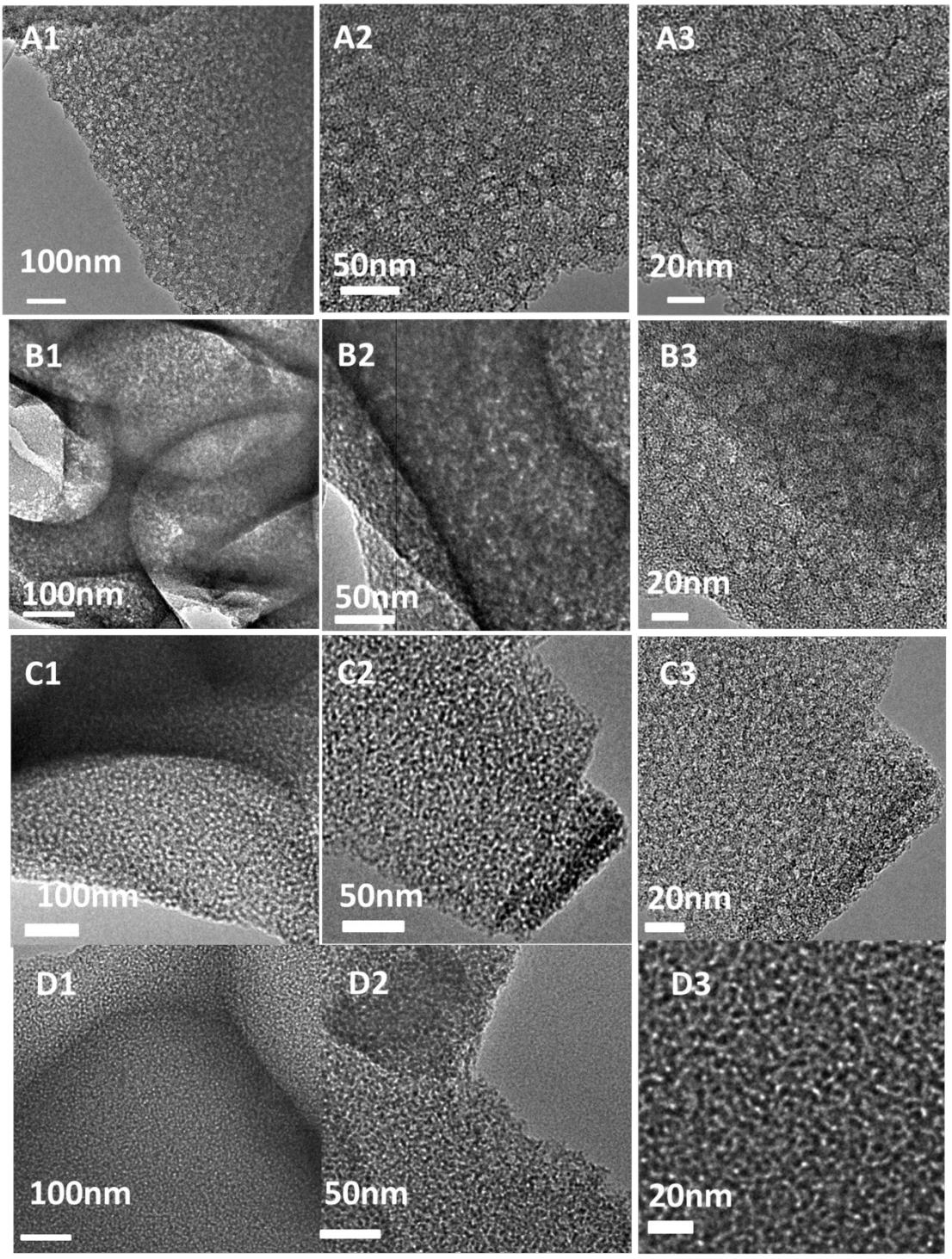

Figure S20. TEM images of $DZ_{0.5}$-C (A1, A2, A3), DZ_1-C (B1, B2, B3), $DZ_{1.5}$-C (C1, C2, C3) and DZ_2-C (D1, D2, D3).

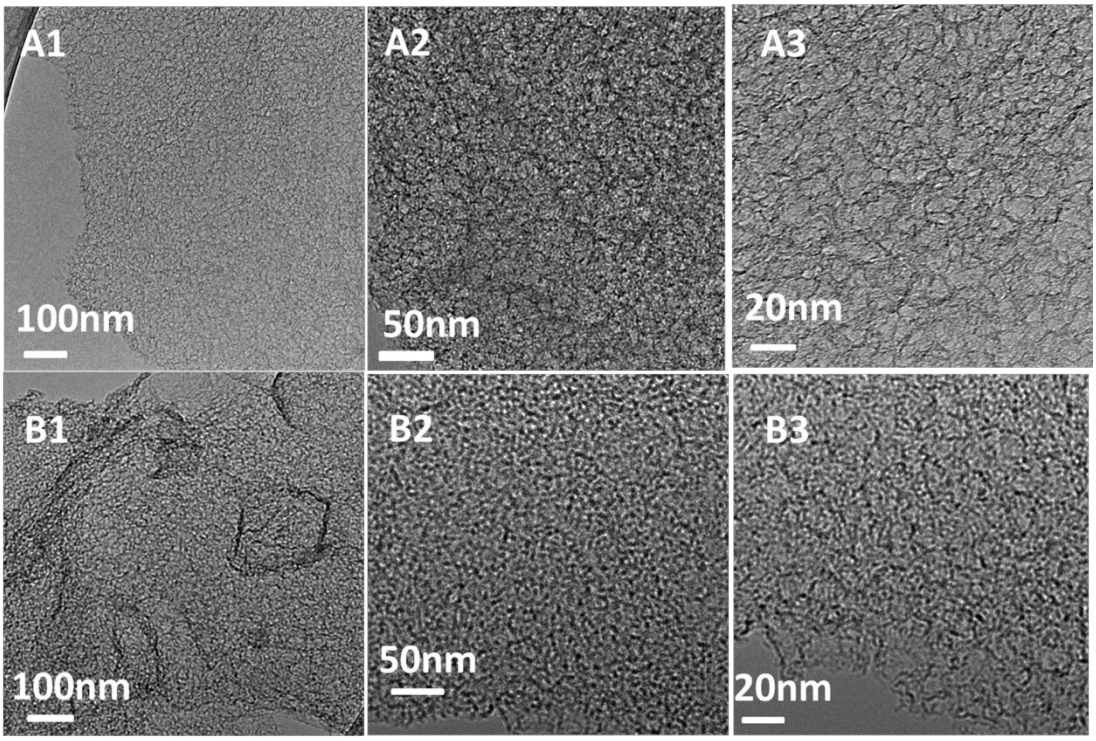

Figure S21. TEM images of $NZ_{0.5}$-C (A1, A2, A3) and NZ_1-C (B1, B2, B3).

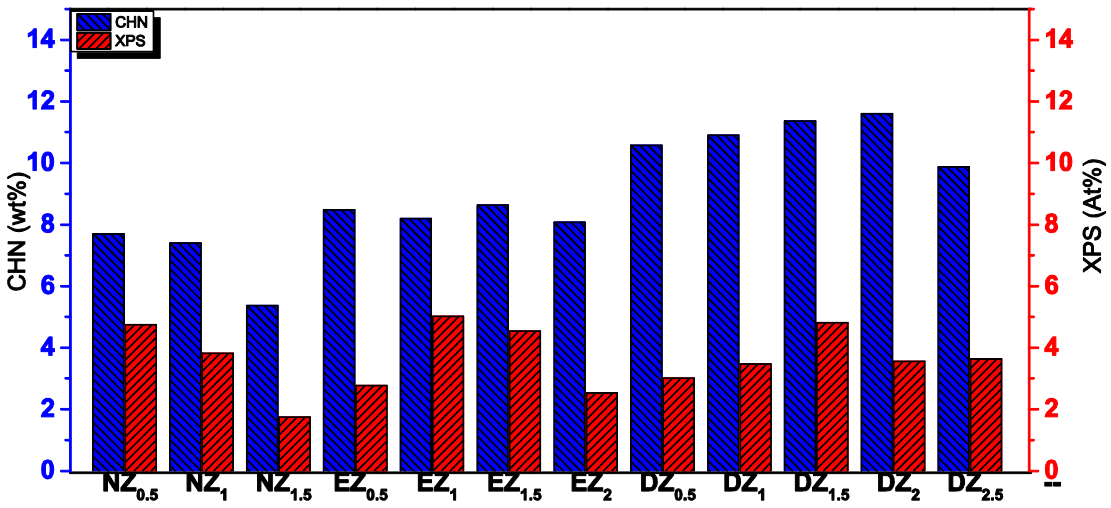

Figure S22. Nitrogen content of NCFs.

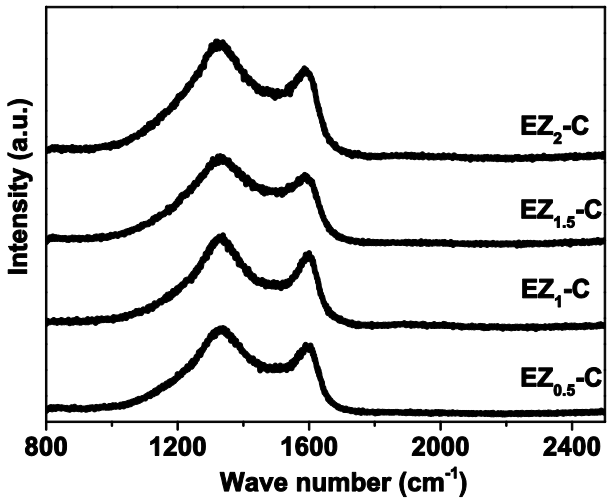

Figure S23. Raman curves of EZ_X-C.

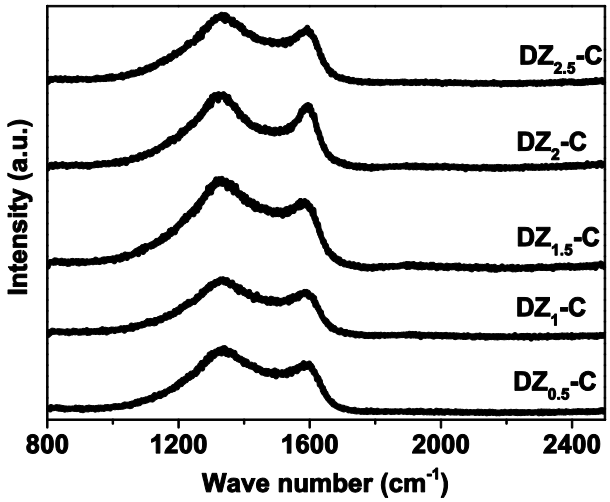

Figure S24. Raman curves of DZ_X-C

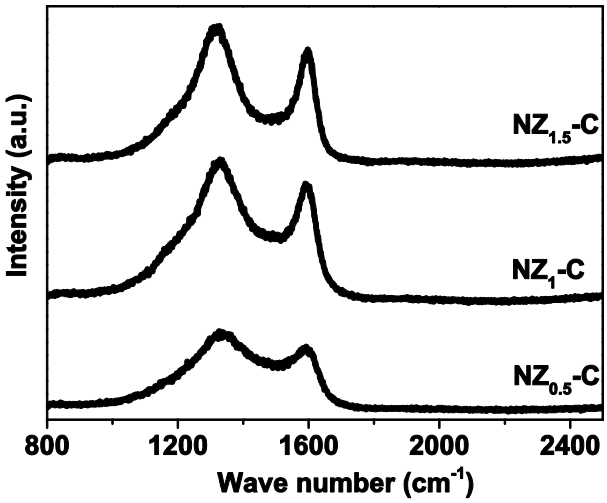

Figure S25. Raman curves of NZ_X-C

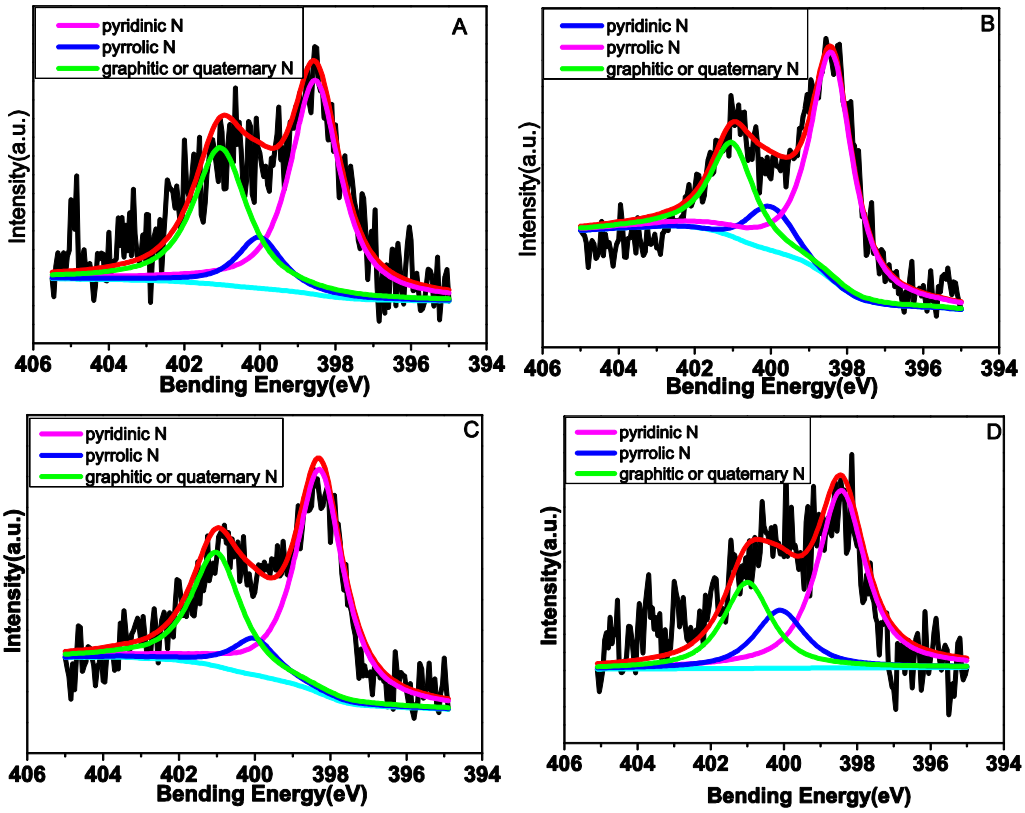

Figure S26. N 1s XPS spectrum of EZ_X-C, A) $EZ_{0.5}$-C, B) EZ_1-C, C) $EZ_{1.5}$-C and D) EZ_2-C.

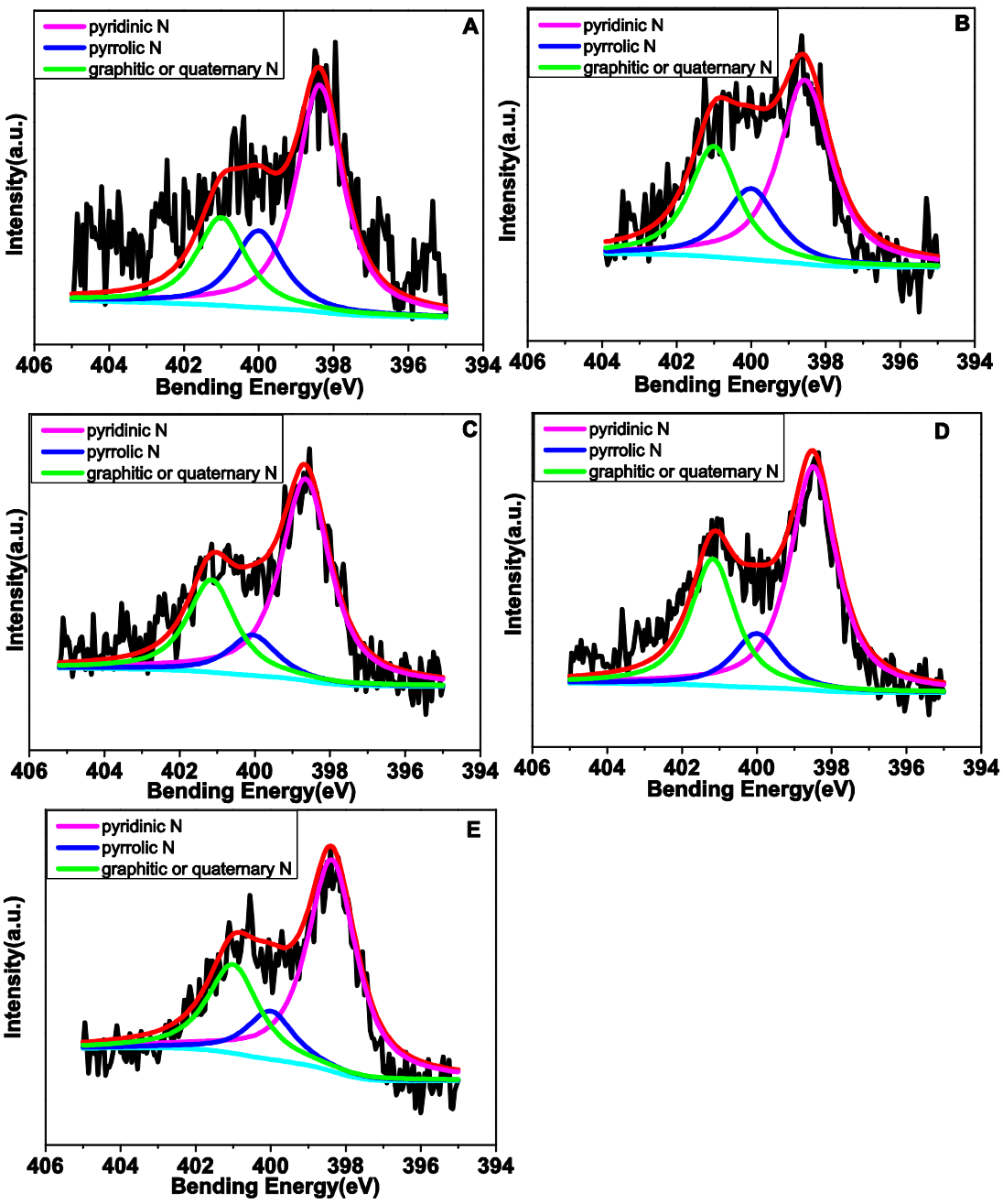

Figure S27. N 1s XPS spectrum of DZ_X-C, A) $DZ_{0.5}$-C, B) DZ_1-C, C) $DZ_{1.5}$-C, D) DZ_2-C and E) $DZ_{2.5}$-C.

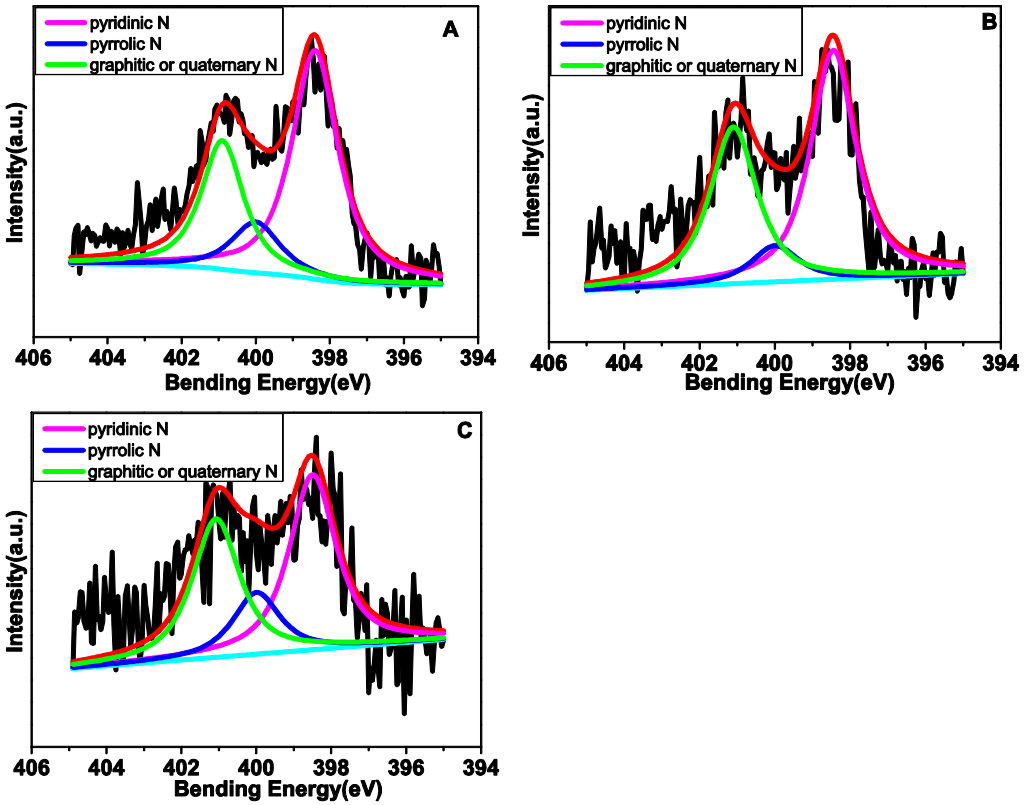

Figure S28. N 1s XPS spectrum of NZ_X-C, A) $NZ_{0.5}$-C, B) NZ_1-C and C) $NZ_{1.5}$-C.

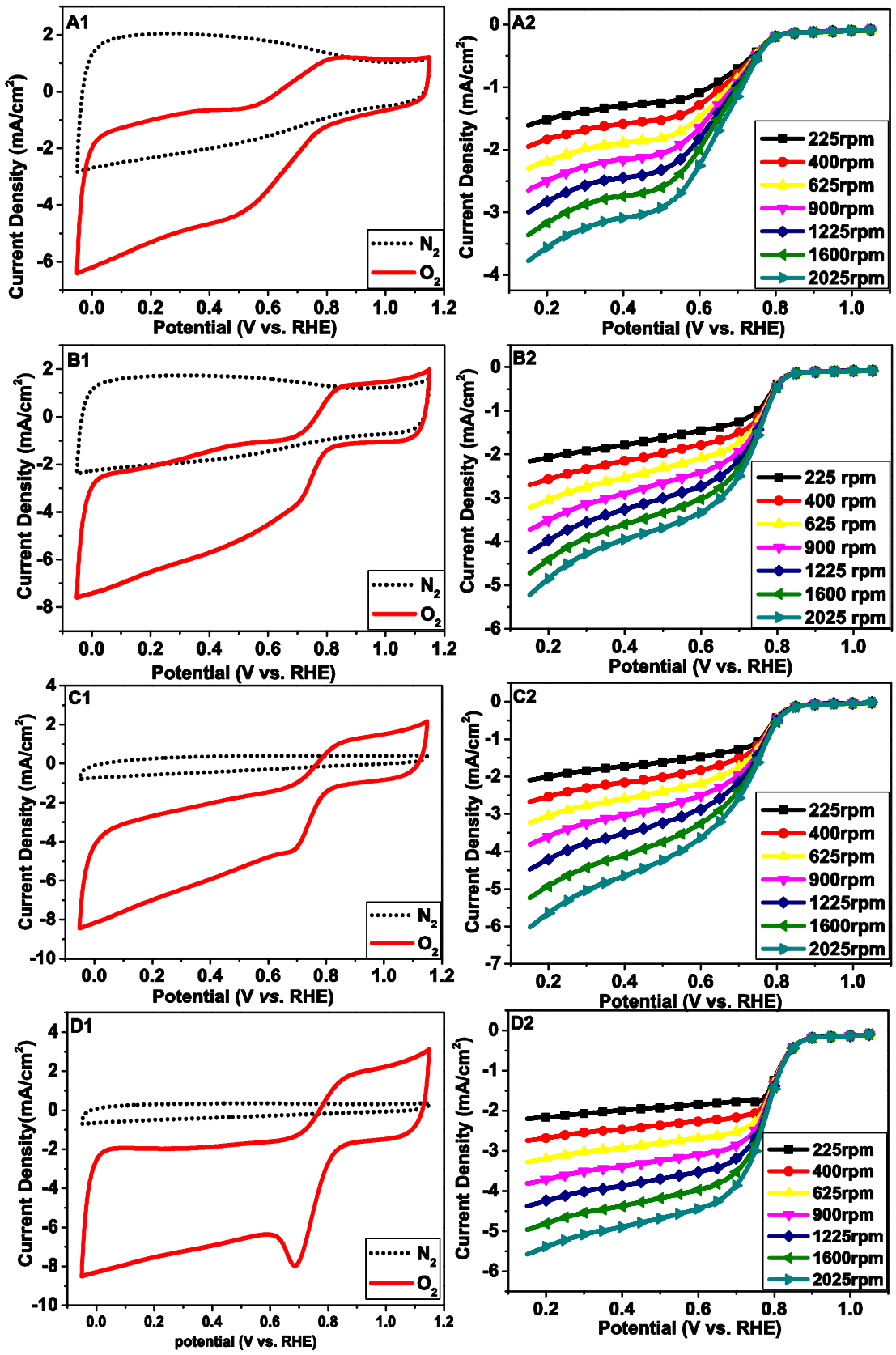

Figure S29. CV and LSV curves of EZ_X-C, A1, A2 ($EZ_{0.5}$-C), B1, B2 (EZ_1-C), C1, C2 ($EZ_{1.5}$-C) and D1, D2 (EZ_2-C).

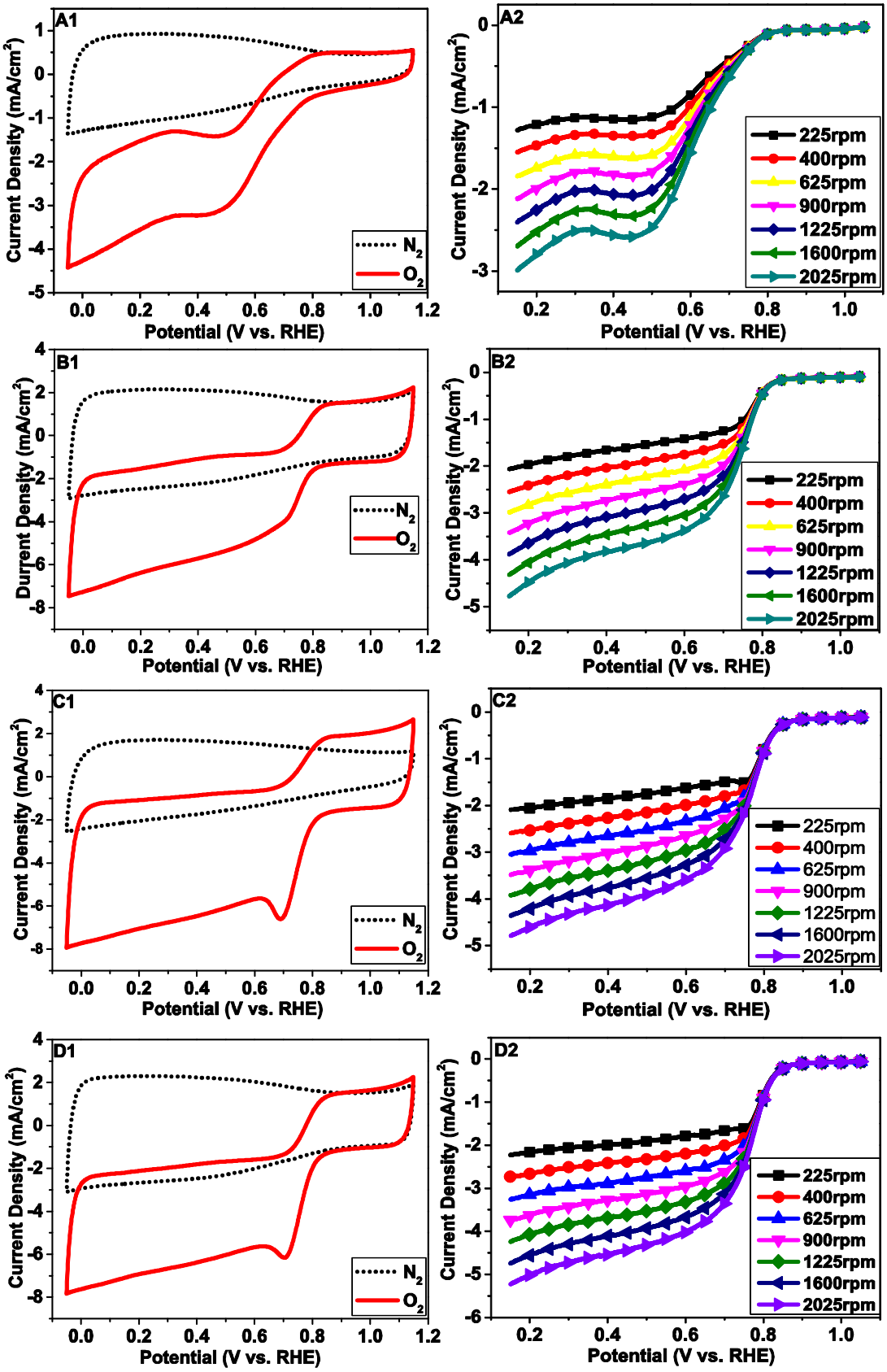

Figure S30. CV and LSV curves of DZ_X-C, A1, A2 ($DZ_{0.5}$-C), B1, B2 (DZ_1-C), C1, C2 ($DZ_{1.5}$-C) and D1, D2 (DZ_2-C).

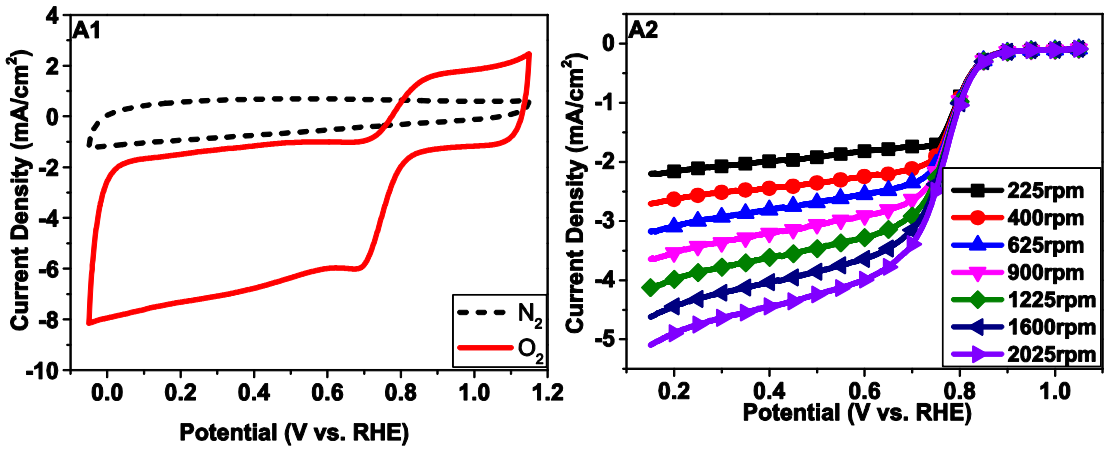

Figure S31. CV and LSV curves of $DZ_{2.5}$-C.

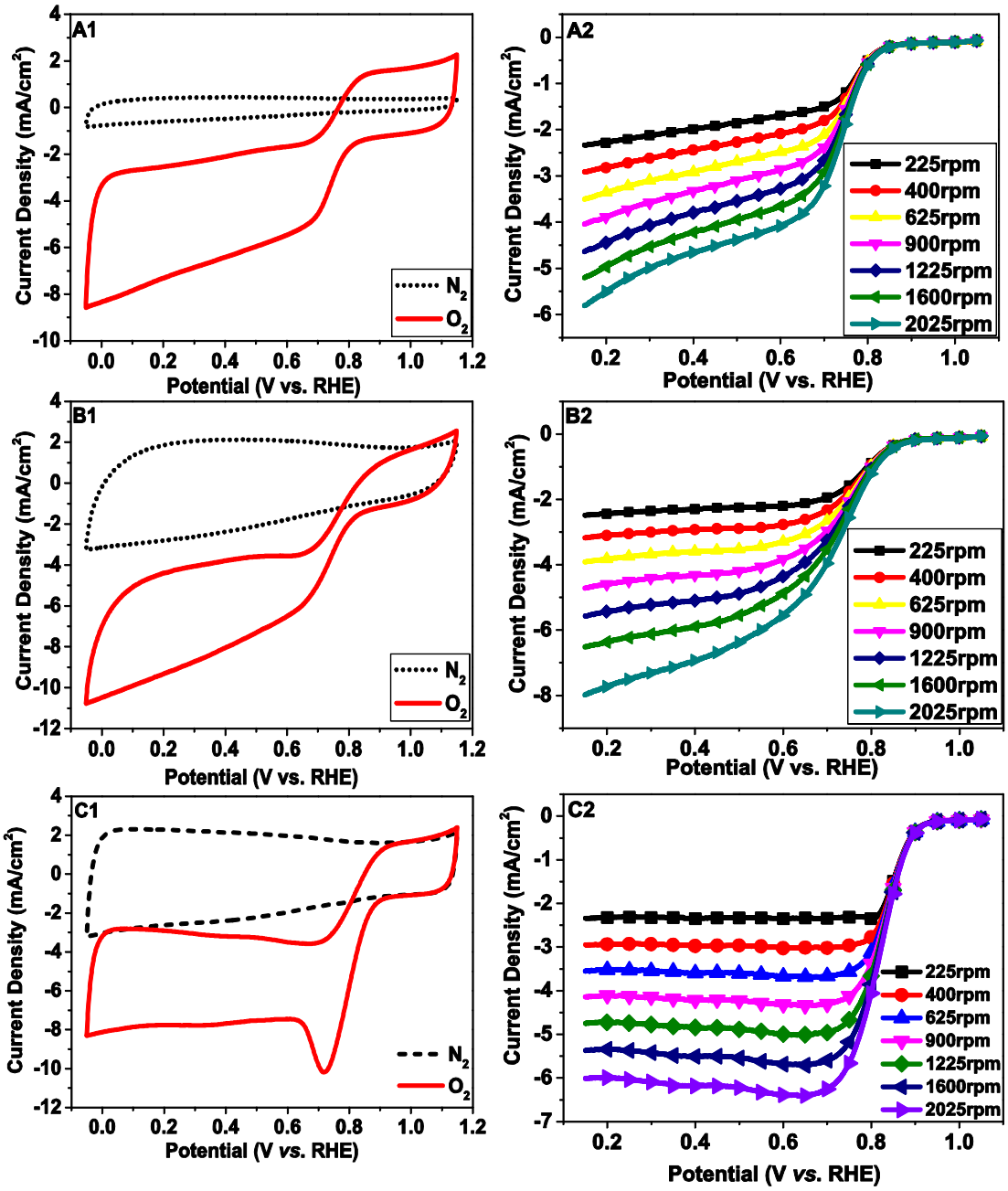

Figure S32. CV and LSV curves of NZ_X-C, A1, A2 ($NZ_{0.5}$-C), B1, B2 (NZ_1-C) and C1, C2 ($DZ_{1.5}$-C).

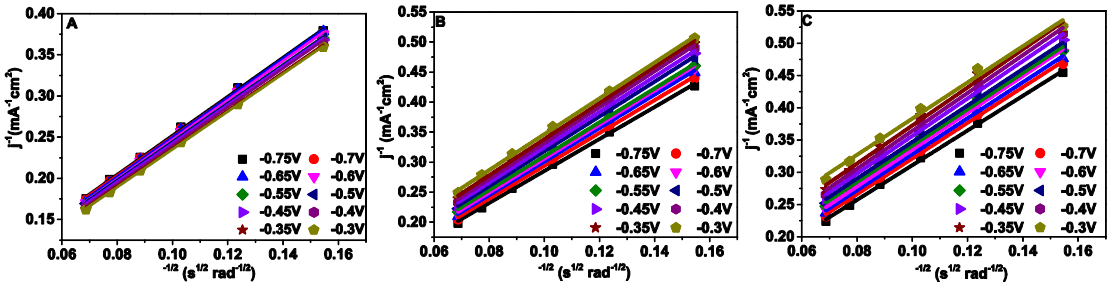

Figure S33. Koutecky-Levich plots at different potentials of A) $NZ_{1.5}$-C, B) EZ_2-C, C) $DZ_{2.5}$-C.

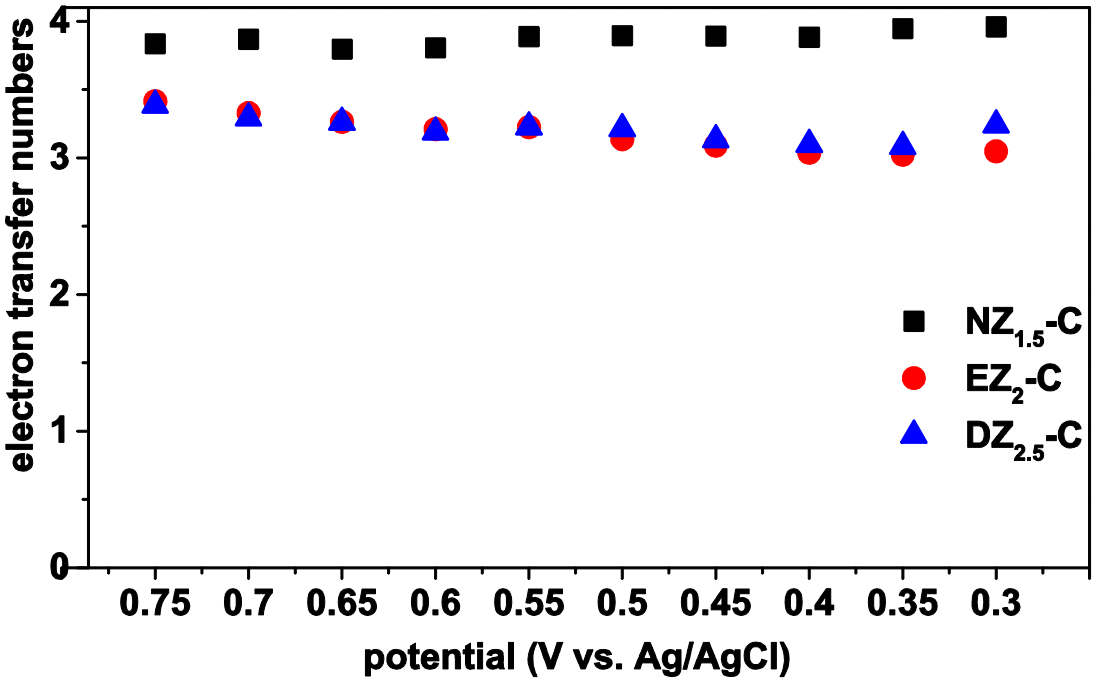

Figure S34. Electron transfer numbers calculated from K-L plots.